JOC The Journal of Organic Chemistry

Article

pubs.acs.org/joc

Carbenoid Alkene Insertion Reactions of Oxiranyllithiums

Lawrence M. Pratt,[†] Binh Khanh Mai,[‡,§] and B. Ramu Ramachandran*[,§]

[†]Department of Physical, Environmental, and Computer Sciences Medgar Evers College, The City University of New York, 1650 Bedford Avenue, Brooklyn, New York 11225, United States

[‡]Institute for Computational Science and Technology, Quarter 6, LinhTrung Ward, Thu Duc District, Ho Chi Minh City, Vietnam

[§]College of Engineering & Science, Louisiana Tech University, Ruston, Louisiana 71272, United States

Supporting Information

ABSTRACT: The first computational investigations of the carbenoid reactions of α-lithiated dimethyl ether (methoxymethyllithium) and the intramolecular and intermolecular reactions of lithiated epoxides with the alkene double bond to yield cyclopropane rings are presented. These reactions represent the full spectrum of known carbenoid pathways to cyclopropanation. The reaction of $Li-CH_2-O-CH_3$ with ethylene proceeds exclusively through a two-step carbolithiation pathway, the intramolecular reaction of 1,2-epoxy-5-hexene follows either the carbometalation or a concerted methylene transfer pathway (the former is energetically more favorable), and the reaction of lithiated ethylene oxide (oxiranyllithium) with ethylene, the main focus of this paper, appears to proceed exclusively by the methylene transfer mechanism. In the case of these latter reactions, the free energy of activation for cyclopropanation tends to decrease with the higher aggregation states. Formation of tetramers or higher aggregates is favorable in nonpolar solvents, but in strongly coordinating solvents such as tetrahydrofuran (THF), steric factors appear to limit aggregate sizes to the dimer. In the case of 1,2-epoxy-5-hexene, consideration of competing reaction pathways provide an explanation for the observed product distribution.

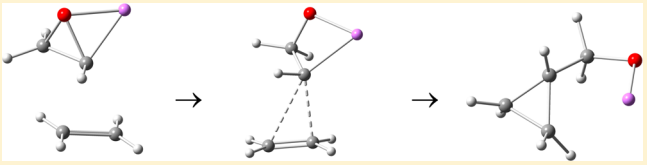

INTRODUCTION

Oxiranyllithiums, which are lithiated epoxides, are intermediate between carbenoids and stabilized carbanions in their chemical properties.[1,2] It has been recognized since at least the 1960s that this intermediate character gives rise to a rich chemistry.[3−7] They undergo carbanion-like reactions with electrophiles,[8] and the chemical and configurational stability of the oxiranyl anion has been exploited for organic synthesis.[9,10] Hydrogen shift and rearrangement reactions have been reported,[3] and in several cases, more than one product is formed.[3−7,11−13] Numerous examples of C−H insertion reactions have also been reported.[1,14−16]

At the same time, carbenoid reactivity has also been observed in oxiranyllithiums. Of particular interest are alkene insertion reactions, resulting in cyclopropane rings. Several *intramolecular* cyclopropanation reactions of oxiranyllithiums have been reported.[17−22] In a recent paper,[23] we reported computational estimates of the free energies for activation $\Delta G^{\ddagger}$ and reaction $\Delta_r G^{\circ}$ for the *intermolecular* reaction of oxiranyllithium with ethylene in nonpolar solvents as well as the polar solvent tetrahydrofuran (THF). The emphasis on that paper, however, was the relative performance of various DFT functionals in reproducing the thermodynamic properties compared to correlated wave function methods such as second-order Møller−Plesset theory, MP2, and coupled cluster theory with perturbative triple excitations, CCSD(T).

In the present paper, our main goal is to present an analysis of the carbenoid reactions of lithiated ethylene oxide aggregates toward ethylene. The small size of this system allows us to study the effects of aggregation and explicit solvation by THF on the reactivity. For completeness and for comparison, we begin with a computational study of the reactions of the α-lithioether CH_3-O-CH_2-Li with ethylene, both in the gas phase and in THF. The intramolecular cyclopropanation reaction of 1,2-epoxy-5-hexene is studied next. In this case, computational consideration of competing reactions are shown to account for the observed distribution of products in the experiments of Hodgson et al.[19] In the case of the simplest oxiranyllithium, i.e, lithiated ethylene oxide, we also report on the effects of aggregation and THF solvation on the carbenoid reactivity. To the best of our knowledge, the present paper represents the first report of computational studies of these reactions.

The lithiated reagents considered in this work are produced as shown in Scheme 1, where the lithium ion is supplied by organolithium reagents such as tertiary butyllithium or lithium tetramethylpiperidide.

The carbenoid reaction of the α-lithiated dimethyl ether with ethylene could proceed through a concerted methylene transfer mechanism or a stepwise carbolithiation mechanism, as shown in Scheme 2. Similarly, two pathways are available to the intramolecular reaction of 1,2-epoxy-5-hexene to form a bicyclic product, as shown in Scheme 3.

Received: July 26, 2012
Published: September 17, 2012

   dx.doi.org/10.1021/jo301550y | J. Org. Chem. 2012, 77, 8605−8614

Scheme 1

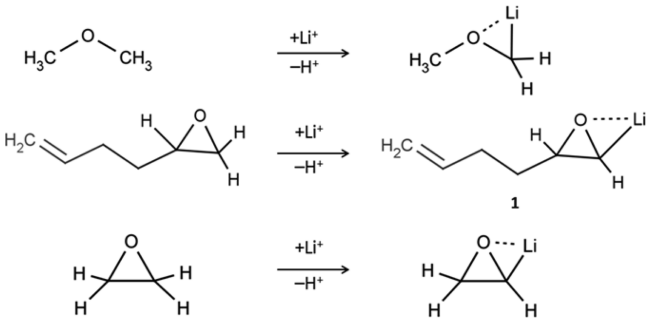

Scheme 2

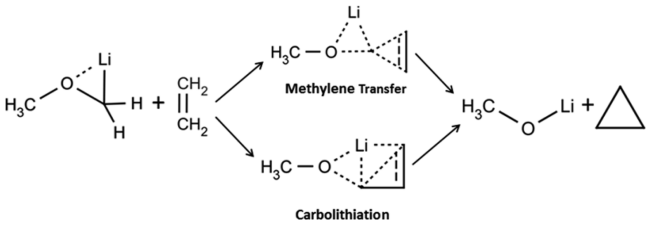

Finally, the main focus of this paper, including the examination of the effects of aggregation and THF solvation, is on the carbenoid reactions of lithiated ethylene oxide, which are summarized in Scheme 4.

We have recently studied the cyclopropanation reactions of halomethyllithiums (X−CH_2−Li; X = F, Cl, Br) with ethylene and 2,3-dimethylbutene.[24,25] In the case of halomethyllithiums, aggregation was shown to have a profound impact on the preferred reaction pathway for methylene insertion into an alkene double bond.[23,24,26] In that case, computations clearly established that aggregated forms of the reagent were the dominant species in solution and that, in sharp contrast to monomers, they showed a strong preference for the concerted methylene transfer pathway over the stepwise carbometalation pathway, thus solving a puzzle that had persisted since the early days of the Simmon−Smith reaction.[27−32] Aggregation, in the case of halomethyllithiums, lowered the reaction barrier for the methylene transfer pathway while dramatically increasing the reaction barrier for the carbometalation pathway. The present studies also provide us with an opportunity to compare the cyclopropanation reaction mechanisms and barrier heights for the carbenoid reactions of oxiranyllithiums with those of the well-studied reactions of halomethyllithiums.

Scheme 4

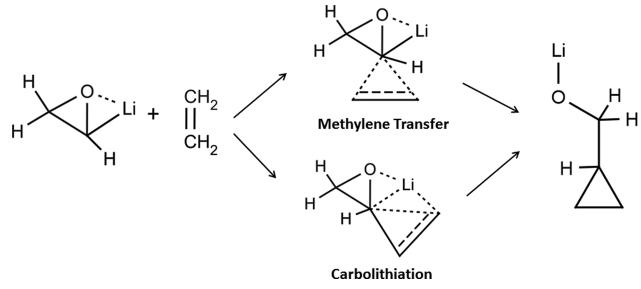

The remainder of this paper is organized as follows. The next section describes the computational methods and methodology adopted in this study. This is followed by a section in which we present the results. The results are discussed and compared to cyclopropanation reactions of halomethyllithium carbenoids in the subsequent section. The final section offers a summary of the main findings and conclusions.

COMPUTATIONAL METHODS

All calculations were performed using the Gaussian 09 suite of programs.[33] Calculations were performed for molecules in the gas phase and with explicitly coordinated THF ligands, which are necessary to model reactions in THF solvent.[24] The gas-phase results, with standard-state corrections, can be extended to nonpolar solvents,[24,34] and all free energies reported in this paper use the condensed phase standard states as the reference. No continuum solvation "corrections" were imposed on the THF microsolvated species. Reaction and activation energies were calculated using density functional theory (DFT), specifically the five functionals B3LYP,[35−37] PBE1PBE (or PBE0),[38,39] and the Minnesota functionals[40] M06, M06L, M062X, each with the 6-31+G(d) basis set. Integrals were evaluated with a pruned numerical grid of 99 radial shells and 770 angular points in each shell (grid = 99770), which is denser than the "ultrafine grid" option of Gaussian 09. Geometry optimizations and frequency calculations were also performed at the MP2 level of theory with the same basis set for gas-phase species up to the tetramers. For the gas-phase species, CCSD(T)/6-31+G(d) single-point energies were also calculated at the optimized geometry from each computational method, except for the tetramers.

The free energies of each species in one-step model chemistries [DFT/6-31+G(d) or MP2/6-31+G(d)] were calculated from the energy at the optimized geometry and the thermal correction to the free energies, obtained from a frequency calculation. Free energies for the two-step model chemistries MP2//DFT and CCSD(T)//X, where X = DFT or MP2, were obtained by adding the thermal correction to the free energy calculated at the lower level to the MP2 or CCSD(T) single-point energy.

Scheme 3

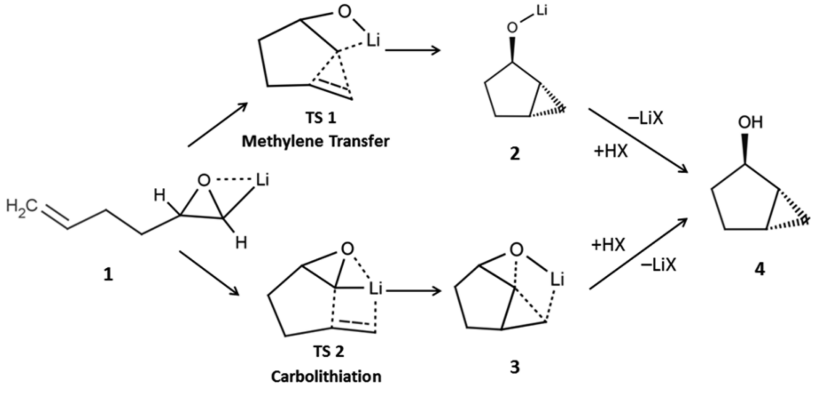

dx.doi.org/10.1021/jo301550y | J. Org. Chem. 2012, 77, 8605−8614

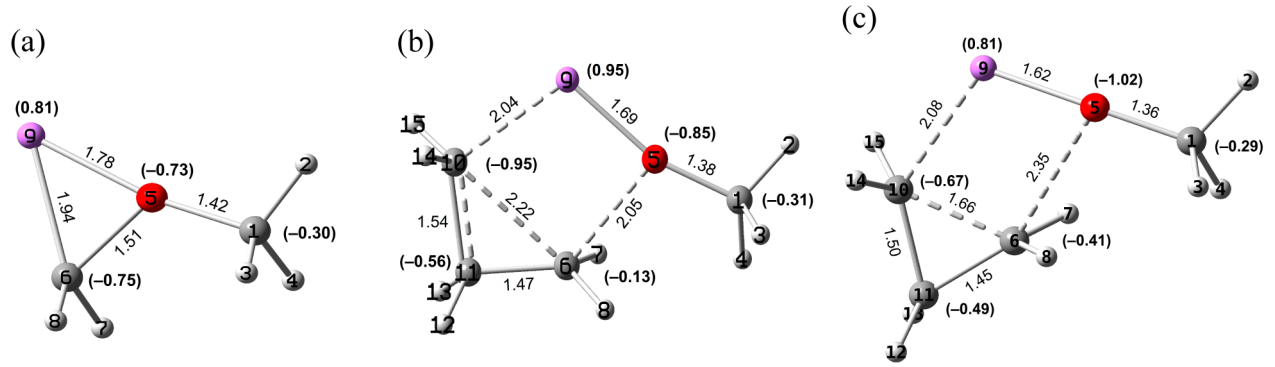

Figure 1. Optimized M06-2X/6-31+G(d) structures for (a) CH_3-O-CH_2-Li, (b) the transition state it forms with ethylene, and (c) a structure along the intrinsic reaction path toward the product at −44.4 kcal/mol relative to the transition state. Lithium is lilac, oxygen is red, carbons are gray, and hydrogens are white. Bond lengths are shown in angstroms and charges from natural population analysis are shown in boldface in parentheses for atoms other than hydrogen.

Table 1. Gibbs Free Energy of Activation $\Delta G^{\ddagger}$ and Reaction $\Delta_r G°$ Relative to Reactants in kcal/mol for the Intermolecular Cyclopropanation Reaction of Figure 1 (Scheme 2) and the Intramolecular Cyclization Reactions of Figure 2 (Scheme 3)

	α-lithioether carbolithiation		intramolecular methylene transfer		intermolecular carbolithiation	
method	$\Delta G^{\ddagger}$	$\Delta_r G°$	$\Delta G^{\ddagger}$	$\Delta_r G°(2)$	$\Delta G^{\ddagger}$	$\Delta_r G°(3)$
B3LYP	21.3	−36.6	17.6	−45.9	9.2	−15.8
M06	18.2	−42.4	15.9	−53.4	6.4	−20.9
M06L	15.5	−43.5	17.5	−50.2	7.4	−18.3
M062X	23.6	−39.4	21.3	−52.4	6.7	−21.7
PBE0	17.1	−42.9	17.8	−55.1	4.6	−23.8
MP2	25.7	−42.3	21.5	−54.0	9.3	−21.4
MP2//B3LYP	26.4	−42.8	21.9	−54.3	11.7	−21.7
MP2//M06	25.9	−43.0	21.0	−54.9	11.6	−21.6
MP2//M06L	26.3	−42.5	21.8	−54.6	11.7	−21.4
MP2//M062X	25.5	−43.1	20.5	−55.1	11.7	−22.3
MP2//PBE0	25.1	−42.9	21.0	54.4	11.8	−21.7
CCSD(T)//B3LYP	25.6	−37.5	19.3	−49.1	11.9	−18.4
CCSD(T)//M06	25.6	−37.6	19.0	−49.7	9.2	−18.4
CCSD(T)//M06L	25.7	−37.1	19.2	−49.3	9.3	−18.1
CCSD(T)//M062X	26.0	−37.7	20.3	−49.9	9.2	−19.0
CCSD(T)//PBE0	25.0	−37.6	18.5	−49.2	9.2	−18.5
CCSD(T)//MP2	26.5	−36.8	22.2	−48.7	9.3	−18.1
$(\langle\Delta G°\rangle \pm \sigma)_{DFT}$	19.2 ± 3.3	−41.0 ± 2.9	18.0 ± 2.0	−51.4 ± 3.5	6.9 ± 1.7	−20.1 ± 3.1
$(\langle\Delta G°\rangle \pm \sigma)_{MP2//DFT}$	25.8 ± 0.5	−42.9 ± 0.2	21.3 ± 0.6	−54.7 ± 0.3	11.7 ± 0.1	−18.5 ± 0.3
$(\langle\Delta G°\rangle \pm \sigma)_{CC//DFT}$	25.6 ± 0.4	−37.5 ± 0.3	19.3 ± 0.7	−49.5 ± 0.4	9.8 ± 1.2	−21.0 ± 1.6

Intrinsic reaction coordinate (IRC) calculations[41,42] were performed using M06-2X from each transition state to confirm that they connected to the correct reactants and products. Natural population analysis (NPA)[43,44] was used to obtain atomic charges shown in some of the figures.

RESULTS

We first examine the reaction of the α-lithioether CH_3-O-CH_2-Li with ethylene, summarized in Scheme 2. The M06-2X/6-31+G(d) optimized structures for the reactant ether and the transition state formed with ethylene are shown in Figure 1.

The transition state has a four-membered ring structure in which the bond between the methyelene carbon (C6) and the oxygen weakens as the interaction between C6 and the two carbons of ethylene (C10 and C11) strengthens. These structures are strongly suggestive of a carbolithiation pathway. IRC calculations from the transition state in Figure 1b suggest that the reaction proceeds through a barrier-free syn elimination of CH_3-O-Li to form cyclopropane, as shown in Figure 1c. The free energies of activation $\Delta G^{\ddagger}$ and free energies of reaction $\Delta_r G°$ for this reaction in a nonpolar solvent are tabulated in Table 1. Also shown are the average values calculated from each class of methods and associated standard deviations.

Atomic charges from NPA are shown for atoms other than hydrogen in Figure 1. These suggest that the role of the lithium in the carbometalation pathway is to polarize the ethylene bond (natural charges are −0.44 on each carbon of ethylene in isolation; see Figure 3) so that the carbenoid carbon can attack the less negative ethylene carbon. Repeated attempts at finding the transition state for a concerted, or methylene transfer, pathway consistently yielded structures nearly identical to that shown in Figure 1b.

Next, we examine the intramolecular insertion of an oxiranyllithium carbenoid into a double bond, exemplified by the reaction of 1 summarized in Scheme 3. In this case, computations identified the concerted methylene transfer transition state **TS 1** as well as the carbolithiation transition

dx.doi.org/10.1021/jo301550y | J. Org. Chem. 2012, 77, 8605−8614

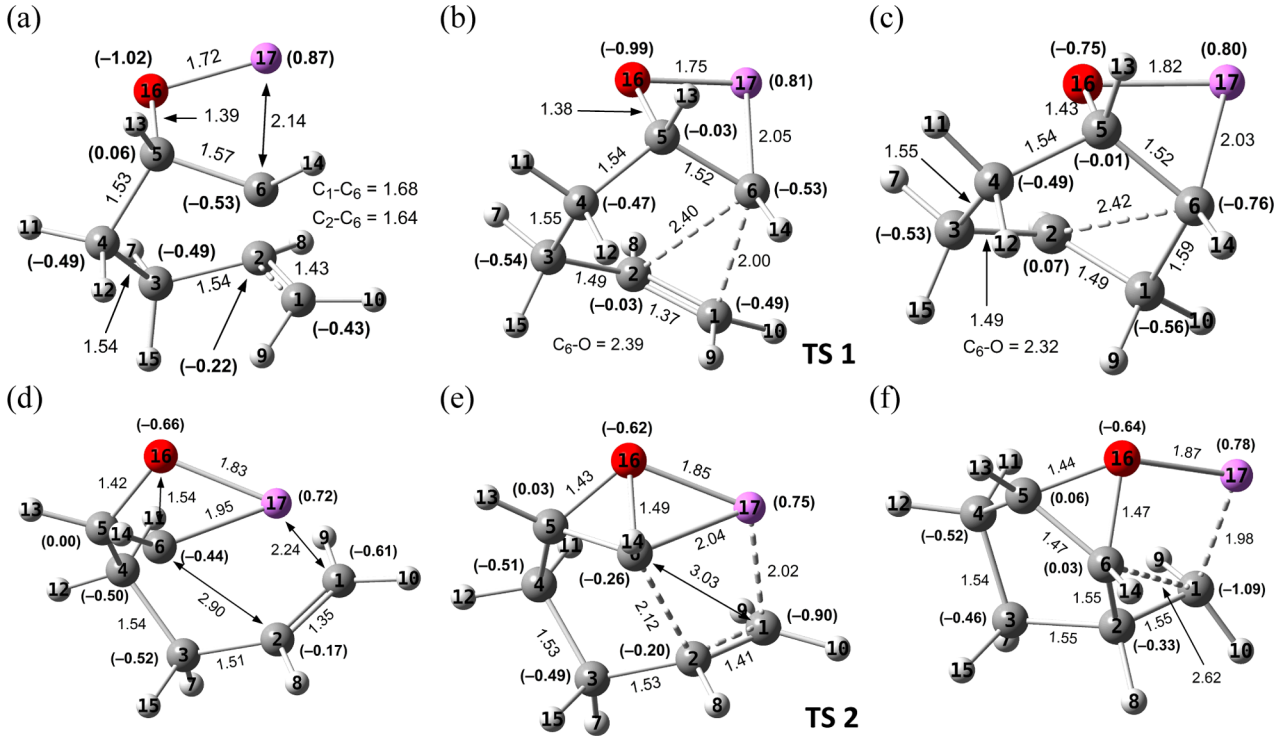

Figure 2. Structures on the M062X intrinsic reaction coordinates for the methylene transfer (top) and carbolithiation (bottom) pathways of the intramolecular carbenoid reaction of lithiated 1,2-epoxy-5-hexene. Panels a and d are structures on the reactant side of the transition states, b and e are transition state structures **TS 1** and **TS 2**, respectively, and c and f are structures on the product side, leading to **2** and **3**, respectively. The convention for atom colors and the numbers shown are the same as those in Figure 1.

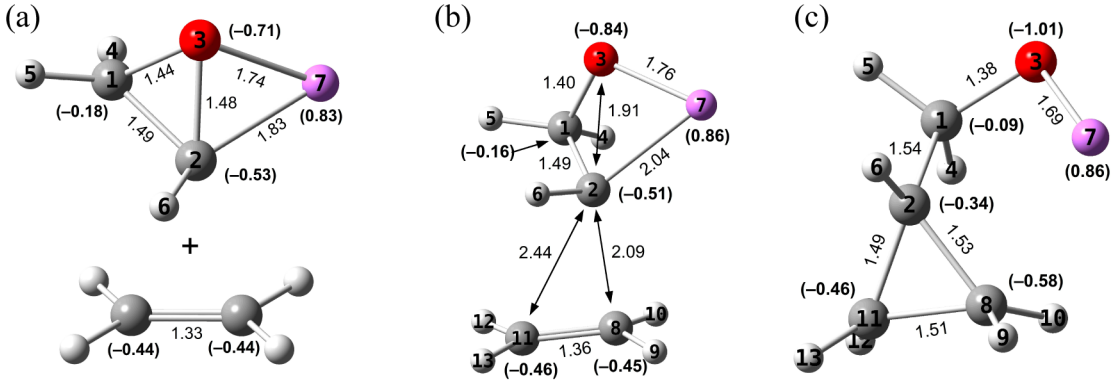

Figure 3. Carbenoid cyclopropanation reaction of the oxiranyllithium monomer with ethylene by the methylene transfer mechanism. M06-2X/6-31+G(d) structures of (a) oxiranyllithium and ethylene (each optimized in isolation), (b) saddle point, and (c) product. The color and numbering conventions are the same as Figure 1.

state **TS 2**. Figure 2 shows structures from the IRCs calculated from each transition state. Complete IRCs for these two pathways are given in the Supporting Information. The free energies of activation and reaction to yield optimized structures **2** or **3**, depending on the reaction path followed, are tabulated in Table 1.

Table 1 indicates that the reaction barrier for the carbolithiation pathway is less than half that of the methylene transfer pathway. Therefore, we conclude that the latter mechanism dominates, especially at lower temperatures. The natural charges in Figure 2 show that, similar to the case of CH_3-O-CH_2-Li, the lithium atom polarizes the double bond, thus facilitating the insertion of the carbenoid carbon into the double bond. The formation of the carbolithiation product **3**, however, is considerably less exoergic than the lithiated alcohol **2**, relative to the reactant **1**. This means that the thermodynamic driving force for the formation of **4** upon final workup of the reaction mixture is greater for **3** than for **2**.

We now turn to the main focus of this paper, namely the intermolecular carbenoid reactions of oxiranyllithium monomers and aggregates with ethylene, shown in Scheme 4. In this case, surprisingly, the reaction appears to proceed exclusively through the concerted methylene transfer pathway. Optimized structures corresponding to the reactant, saddle point, and product in the intermolecular reaction of the oxiranyllithium monomer are shown in Figure 3. The C2−O distance in the transition state increases to 1.91 Å while the C1−C2 distance remains unchanged from the reactant structure and the C1−O and O3−Li distances change only by small amounts, suggesting that this might be an "early" transition state. The averages and

dx.doi.org/10.1021/jo301550y | J. Org. Chem. 2012, 77, 8605−8614

Table 2. Activation and Reaction Free Energy Changes (kcal/mol) for the Concerted Reaction of Lithioethylene Oxide with Ethylene

	ΔG°_{MP2}	$\Delta G^\circ_{CC//MP2}$	$(\langle\Delta G^\circ\rangle \pm \sigma)_{DFT}$	$(\langle\Delta G^\circ\rangle \pm \sigma)_{MP2//DFT}$	$(\langle\Delta G^\circ\rangle \pm \sigma)_{CC//DFT}$
$\Delta G^\ddagger$	20.2	19.5	18.0 ± 2.1	19.1 ± 0.3	20.0 ± 0.3
$\Delta_r G^\circ$	−52.6	−53.0	−51.9 ± 3.9	−48.2 ± 0.3	−52.0 ± 2.5

standard deviations of the associated free energy changes, calculated at the various levels of theory mentioned above, are tabulated in Table 2. The complete table is provided in Supporting Information.

Multiple attempts were made to identify a transition state for the carbolithiation pathway in Scheme 4 using various computational strategies. However, these consistently led to structures whose imaginary frequencies corresponded to a 1,2 hydrogen transfer between the two carbons. The M06-2X/6-31+G(d) hydrogen transfer transition state structure for the intermolecular cases are shown in Figure 4a, with a $\Delta G^\ddagger$ = 20.3

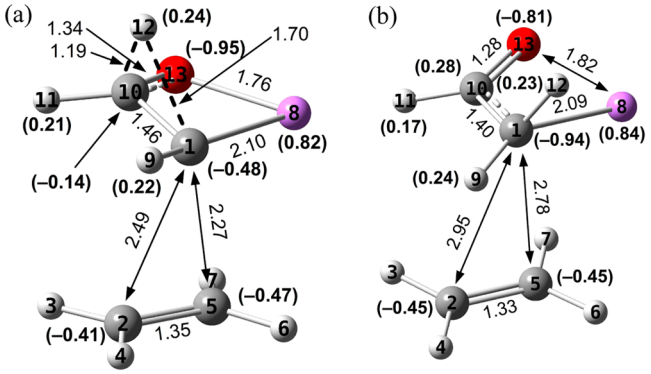

Figure 4. Transition state structure ($\Delta G^\ddagger$ = 20.3 kcal/mol) for the 1,2 hydrogen transfer (left) of an oxiranyllithium, and (right) the "product" structure found by following the intrinsic reaction coordinate toward the product side until the energy drops 55.2 kcal/mol below the transition state. The imaginary frequency corresponds to migration of H12 from C10 to C1, resulting in isomerization to the ketone. Natural charges on the hydrogens H9, H11, and H12 in addition to those on the non-hydrogen atoms are shown in parentheses in boldface.

kcal/mol. Following the IRC toward the products from this transition state yields the lithiated aldehyde structure shown in Figure 4b, at −55.2 kcal/mol relative to the transition state. The natural charges in the transition state show that the ethylene C5 and the carbenoid C1 have comparable charges. However, the carbenoid C1, to which the hydrogen migrates, acquires a distinct carbanion characteristic on the product side of the IRC.

The role of ethylene in this reaction is interesting. The natural charges shown in Figure 4b for the ethylene carbons are almost identical to those in free ethylene (compare with Figure 3a), suggesting that interaction of the oxiranyllithium with ethylene is weak. Moreover, in the absence of ethylene, the M06-2X/6-31+G(d) free energy barrier for hydrogen transfer increases only by a modest amount, to 21.4 kcal/mol. However, in this latter scenario, either of the two hydrogens on C10 may transfer while, in the presence of ethylene, only the hydrogen on the "far side" of the double bond migrates.

We also examined the reaction of THF-solvated CH_3-O-CH_2-Li with ethylene by placing two THF ligands on the lithium atom. Table 3 summarizes the free energy changes for

Table 3. Activation and Reaction Free Energies for THF-Solvated α-Lithio Dimethyl Ether

	ΔG°_{MP2}	$(\langle\Delta G^\circ\rangle \pm \sigma)_{DFT}$	$(\langle\Delta G^\circ\rangle \pm \sigma)_{MP2//DFT}$
$\Delta G^\ddagger$	31.3	22.4 ± 3.8	24.6 ± 0.6
$\Delta_r G^\circ$	−47.2	−48.5 ± 2.7	−50.6 ± 0.4

each class of methods used. As in the case of Table 2, the complete table is provided in Supporting Information. Comparing Table 3 to Table 1, we see that there is a significant increase in the MP2 barrier height in THF solution, and a significant increase in the exoergicity of the reaction. However, the MP2 barrier is substantially higher than those from DFT and MP2//DFT calculations. We have verified that the transition state structures from MP2 and DFT as well as the imaginary vibrational modes from each method are qualitatively similar. Therefore, the discrepancy cannot be attributed to qualitative differences in the structures identified by the two classes of methods. There is considerable spread in the $\Delta G^\ddagger_{DFT}$; both B3LYP and M06-2X predict barriers of 26 kcal/mol while M06L predicts 17 kcal/mol. Despite this spread, the MP2//DFT reaction barriers are highly consistent, as indicated by the small standard deviation. Turning to reaction free energies, it is clear that THF solvation stabilizes the methoxylithium product, as indicated by the higher exoergicity in THF (Table 3) compared to nonpolar solvents (Table 1).

Prior to discussing the thermodynamics of the reactions of oxiranyllithium aggregates with ethylene, we consider the relative stability of the various aggregate forms in nonpolar solutions and in THF-solvated form. Two diastereomers *RR* and *RS* are possible for the dimers of oxiranyllithium, and three tetrameric forms *RRRR*, *RRRS*, and *RRSS*.[34] Two structural isomers were identified for each of the *RR* and *RS* diastereomers, which we label dimer 1 and dimer 2.

Table 4 summarizes the energy of formation of the dimers and tetramers, *all relative to the monomer*. Thus, for example, the free energy change shown for the dimer is the free energy change for the processes 2 *R* → *RR*, etc. and for the tetramer, 4 *R* → *RRRR*, etc. The CCSD(T) single-point energies were not computed for the tetramers. For the sake of brevity, we report only the average ΔG's for each class of DFT-based methods along with the standard deviations. The complete tables are provided as Supporting Information.

Considering the ΔG°_{MP2} entries in Table 4, we see that the dimers are easily formed with the release of ∼42 kcal/mol of energy, and that the formation of tetramers from the dimers would release an additional ∼22 kcal/mol, calculated as ΔG°_{MP2}(tetramer) − 2 × ΔG°_{MP2}(dimer). The remaining entries in Table 4 are comparable to the corresponding MP2 entries. Thus, all methods predict that tetramers are overwhelmingly favored in nonpolar media.

We now consider the relative stabilities of THF-solvated aggregates. In the monomeric form, the Li atom prefers to coordinate with two THF molecules, giving R·2THF. The free enrergy change for R·3THF → R·2THF + THF is $\Delta_r G^\circ_{MP2//B3LYP}$ = −10.5 kcal/mol, and $\Delta_r G^\circ_{MP2//M06\text{-}2X}$ =

dx.doi.org/10.1021/jo301550y | J. Org. Chem. 2012, 77, 8605−8614

Table 4. Free Energy Changes $\Delta G°$ for Forming the Aggregates from the Monomer (kcal/mol)

method	dimer 1 *RR*	dimer 2 *RR*	dimer 1 *RS*	dimer 2 *RS*	*RRRR*	*RRRS*	*RRSS*
$\Delta G°_{MP2}$	−43.0	−42.1	−43.0	−41.8	−107.1	−107.7	−107.7
$\Delta G°_{CC//MP2}$	−43.3	−42.3	−43.4	−42.1	–	–	–
$(\langle\Delta G°\rangle \pm \sigma)_{DFT}$	−41.6 ± 1.9	−41.0 ± 1.8	−41.8 ± 1.8	−40.8 ± 1.8	−103.2 ± 6.9	−102.7 ± 7.0	−100.9 ± 6.1
$(\langle\Delta G°\rangle \pm \sigma)_{MP2//DFT}$	−42.8 ± 0.4	−42.1 ± 0.1	−43.2 ± 0.1	−41.9 ± 0.2	−107.0 ± 0.8	−107.1 ± 0.4	−104.2 ± 1.2
$(\langle\Delta G°\rangle \pm \sigma)_{CC//DFT}$	−43.1 ± 0.4	−42.3 ± 0.1	−43.5 ± 0.1	−42.2 ± 0.2	–	–	–

Table 5. Free-Energy Changes $\Delta G°$ (kcal/mol) for the Formation of THF-Solvated Dimers from Disolvated Monomers R·2THF

	dimer 1				dimer 2			
	RR·2THF	RS·2THF	RR·4THF	RS·4THF	RR·2THF	RS·2THF	RR·4THF	RS·4THF
$\Delta G°_{MP2}$	−9.2	−9.1	–	–	−8.8	−10.7	–	–
$\Delta G°_{PBE0}$	−9.4	−8.6	−13.2	−12.7	−7.8	−8.5	−11.6	−13.5
$(\langle\Delta G°\rangle \pm \sigma)_{DFT}$	−6.5 ± 1.6	−6.2 ± 1.6	−17.6 ± 6.0	−17.4 ± 5.6	−5.0 ± 1.6	−6.9 ± 1.2	−15.1 ± 4.7	−16.6 ± 4.7
$(\langle\Delta G°\rangle \pm \sigma)_{MP2//DFT}$	−2.8 ± 4.3	−2.5 ± 4.1	−24.8 ± 2.5	−24.7 ± 2.2	−1.6 ± 4.1	−2.9 ± 3.9	−21.4 ± 1.5	−22.8 ± 1.7
$\Delta G°_{MP2//PBE0}$	−10.2	−9.1	−26.1	−25.1	−8.5	−9.5	−22.5	−23.8

−10.1 kcal/mol. We consider the energetics of forming the disolvated and tetrasolvated dimers, $(R)_2$·2THF and $(R)_2$·4THF, respectively. In Table 5, the free energy change for the formation of these dimers from the disolvated monomers are summarized. Standard state corrections for free THF ligands[24,34] have been applied where necessary. MP2 geometry optimizations were not performed for the tetrasolvated dimers.

Table 5 shows that tetrasolvated dimers are considerably more stable than the disolvated species and, therefore, are expected to be the dominant dimer form in THF solution. Curiously, the $\langle\Delta G°\rangle_{DFT}$ and $\langle\Delta G°_{MP2//DFT}\rangle$ values in Table 5 are considerably different from $\Delta G°_{MP2}$ and, in the case of the latter average, with large standard deviations. The exception is PBE0 (shown in Table 5), which consistently yielded results in fairly good agreement with MP2, and $\Delta G°_{MP2//PBE0}$ (also shown in Table 5) are also in good agreement with $\Delta G°_{MP2}$. The energetics of the formation of THF-solvated tetramers are tabulated in Table 6. In sharp contrast to nonpolar media, tetrasolvated tetramers are predicted to be unstable relative to the tetrasolvated dimers.

Table 6. Reaction Free Energies $\Delta_r G°$ for the Formation of Tetrasolvated Tetramers $(R)_4$·4THF from Tetrasolvated Dimer 1 Molecules

	B3LYP	M06-2X	MP2//B3LYP	MP2//M062X
2 RR·4THF → RRRR·4THF + 4THF	15.8	17.1	30.7	44.7
RR·4THF + RS·4THF → RRRR·4THF + 4THF	16.0	19.5	19.5	45.2
2 RR·4THF → RRSS·4THF + 4THF	15.4	17.2	30.7	46.6
2 RS·4THF → RRSS·4THF + 4THF	16.2	18.5	31.4	46.7

Thus, it appears that in nonpolar media, oxiranyllithium exists predominantly as the tetramer while in THF solution, available evidence suggests that the tetrasolvated dimer is the most stable species. We now consider the reaction thermodynamics of oxiranyllithium aggregates with ethylene in nonpolar and THF solution.

The structures relevant for the reactions of the *RR* dimers are shown in Figure 5, and those for the *RS* dimers in Figure 6. The free energies of activation for these species are summarized in Table 7. In Table 7, we also include the $\langle\Delta G^{‡}\rangle_{MP2//DFT}$ values for the tetrameric species. The free energies of activation for the four dimeric species are quite similar and comparable to the barriers predicted for the monomer. The variations among the MP2//DFT and CCSD(T)//DFT model chemistries are very small, as indicated by the low standard deviations, and the respective averages agree well with the MP2 and CCSD(T)//MP2 predictions quite well.

Turning to the tetramers in Table 7, we note that the $\Delta G^{‡}$ are predicted to be smaller than those for the dimers on average, and that the barrier for the *RRSS* tetramer is especially smaller than the other species. We did not perform CCSD(T) calculations on the tetramers because the 34-atom transition state structure was computationally intractable. The *smallest* $\langle\Delta G^{‡}\rangle_{MP2//DFT}$ values for the monomer, dimers, and tetramers are thus 19.1 ± 0.3 (Table 2), 16.3 ± 0.6 (*RS* dimer 2; Table 7), and 11.6 ± 1.0 (*RRSS*; Table 7) kcal/mol.

Table 8 summarizes the reaction energies $\Delta_r G°$ for the dimeric species. The free energies of reaction tabulated in Table 8 indicate that, similar to the case of the $\Delta G^{‡}$, the reaction free energies $\Delta_r G°$ computed by various methods for the dimeric species are also very similar. The rather large standard deviations in $\langle\Delta_r G°\rangle_{DFT}$ are caused primarily by B3LYP, which predicts a less exoergic reaction for all four dimers, as shown in Table S5A of the Supporting Information. The pattern is repeated in the CCSD(T)//B3LYP results (but not MP2//B3LYP) with the result that the standard deviation for the CCSD(T)//DFT model chemistries in this case are nearly as large as those for the DFT methods. Comapring these results to Table 2 for the reaction of the monomeric species, it appears that the stabilization of the product by the monomeric fragment remaining after cyclopropanation leads to significantly more exoergic reactions in the case of the dimers.

We now consider the thermodynamics of the cyclopropanation reactions of the THF-solvated oxiranyllithium species. Explicit coordination of the THF ligands rapidly increase the size of the molecular system (13 atoms per THF), and therefore we report optimized geometries and free energy corrections only at DFT levels of theory and also calculate MP2//DFT energies for dimeric species with two THF

dx.doi.org/10.1021/jo301550y | J. Org. Chem. 2012, 77, 8605−8614

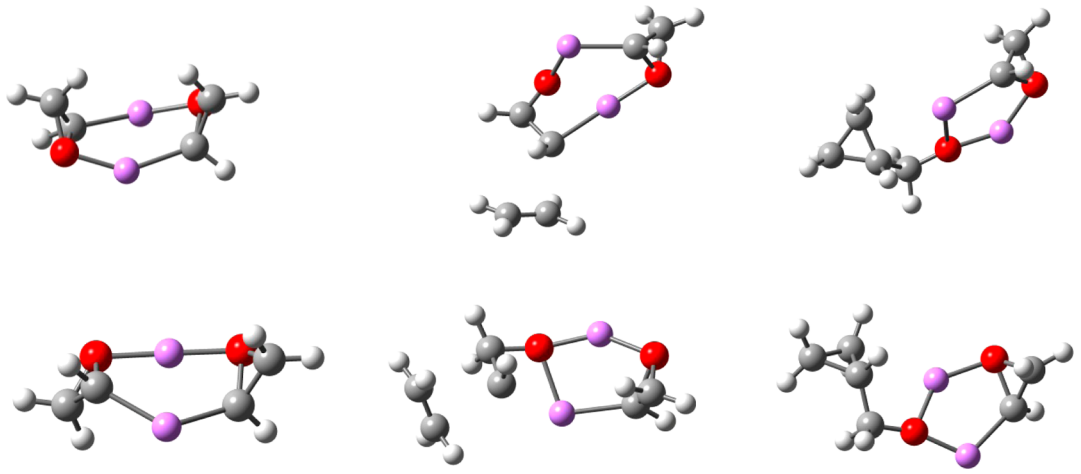

Figure 5. Structures relevant for the gas-phase reaction of the oxiranyllithium RR dimer 1 (top row) and RR dimer 2 (bottom row). Left: oxiranyllithium; center: transition state; right: product.

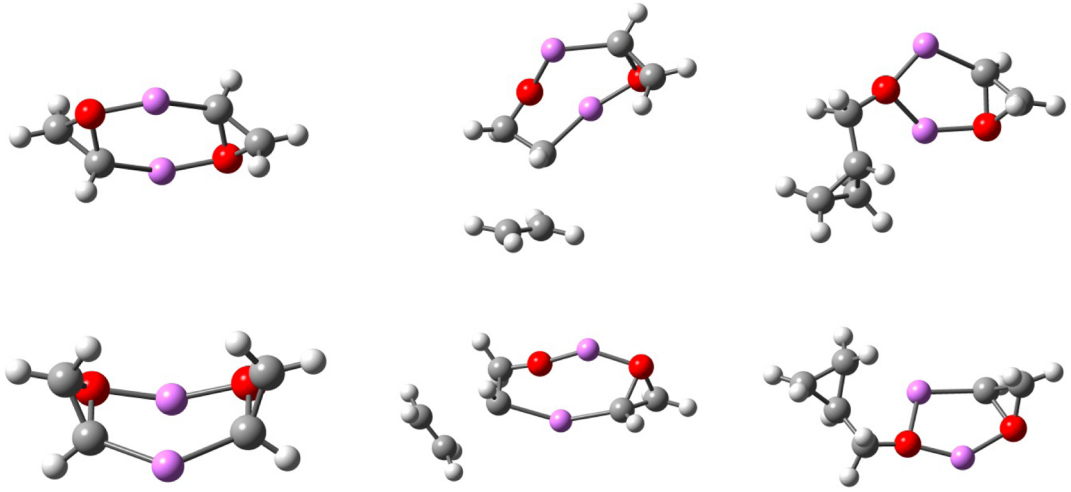

Figure 6. Gas-phase reaction of the oxiranyllithium RS dimer 1 (top row) and RS dimer 2 (bottom row). Left: oxiranyllithium; center: transition state; right: product.

Table 7. Activation Free Energies $\Delta G^{\ddagger}$ of Oxiranyllithium Aggregates for the Cyclopropanation Reaction with Ethylene (kcal/mol) in a Nonpolar Solvent

method	dimer 1 *RR*	dimer 2 *RR*	dimer 1 *RS*	dimer 2 *RS*	tetramer *RRRR*	tetramer *RRRS*	tetramer *RRSS*
MP2	20.0	18.9	20.3	18.6	–	–	–
CCSD(T)//MP2	19.0	17.6	19.1	17.5	–	–	–
$(\langle\Delta G^{\ddagger}\rangle \pm \sigma)_{DFT}$	18.7 ± 2.1	17.8 ± 1.7	19.2 ± 1.8	17.4 ± 1.9	14.5 ± 1.8	13.7 ± 2.0	12.5 ± 1.6
$(\langle\Delta G^{\ddagger}\rangle \pm \sigma)_{MP2//DFT}$	17.5 ± 0.7	16.7 ± 0.7	18.3 ± 0.5	16.3 ± 0.6	16.9 ± 0.5	14.1 ± 0.7	11.6 ± 1.0
$(\langle\Delta G^{\ddagger}\rangle \pm \sigma)_{CC//DFT}$	19.2 ± 0.5	18.6 ± 0.6	20.1 ± 0.6	18.0 ± 0.5			

Table 8. Reaction Free Energies $\Delta_r G°$ in kcal/mol of Oxiranyllithium Cyclopropanation Reaction with Ethylene (kcal/mol) in a Nonpolar Solvent

method	dimer 1 *RR*	dimer 2 *RR*	dimer 1 *RS*	dimer 2 *RS*
MP2	−61.5	−62.5	−61.7	−62.6
CCSD(T)//MP2	−62.3	−63.7	−62.6	−63.5
$(\langle\Delta_r G°\rangle \pm \sigma)_{DFT}$	−60.0 ± 3.5	−60.5 ± 3.4	−59.7 ± 3.4	−60.8 ± 3.4
$(\langle\Delta_r G°\rangle \pm \sigma)_{MP2//DFT}$	−58.1 ± 0.5	−59.3 ± 0.3	−58.1 ± 0.3	−59.1 ± 0.2
$(\langle\Delta_r G°\rangle \pm \sigma)_{CC//DFT}$	−61.6 ± 2.7	−62.6 ± 2.5	−61.4 ± 2.5	−62.5 ± 2.5

molecules per Li atom (i.e., tetrasolvated dimers). Also, having established that the reaction leading to the cyclopropane derivative proceeds by a concerted methylene transfer mechanism, we limit our transition state searches to structures relevant for that case. Once again, we report only the average ΔG's for each class of methods along with the standard

dx.doi.org/10.1021/jo301550y | *J. Org. Chem.* 2012, 77, 8605−8614

Table 9. Activation Free Energies $\Delta G^{\ddagger}$ and Reaction Free Energies $\Delta_r G°$ of Oxiranyllithium Cyclopropanation Reaction with Ethylene (kcal/mol) in THF Solvent[a]

method	monomer	dimer 1 *RR*	dimer 2 *RR*	dimer 1 *RS*	dimer 2 *RS*
$\Delta G^{\ddagger}_{MP2}$	19.4	–	–	–	–
$(\langle \Delta G^{\ddagger} \rangle \pm \sigma)_{DFT}$	18.8 ± 2.3	20.7 ± 2.8	21.2 ± 2.7	18.0 ± 4.4	20.1 ± 3.0
$(\langle \Delta G^{\ddagger} \rangle \pm \sigma)_{MP2//DFT}$	20.2 ± 1.2	21.8 ± 1.6	21.3 ± 0.8	16.7 ± 2.6	20.6 ± 0.6
$\Delta_r G°_{MP2}$	−58.4	–	–	–	–
$(\langle \Delta_r G° \rangle \pm \sigma)_{DFT}$	−54.8 ± 3.2	−59.2 ± 3.8	−59.6 ± 4.0	−60.6 ± 4.6	−60.7 ± 4.3
$(\langle \Delta_r G° \rangle \pm \sigma)_{MP2//DFT}$	−51.5 ± 0.7	−62.3 ± 1.3	−62.3 ± 1.0	−65.0 ± 1.5	−65.1 ± 1.2

[a]Each Li atom in each species listed is solvated by two THF molecules.

Scheme 5

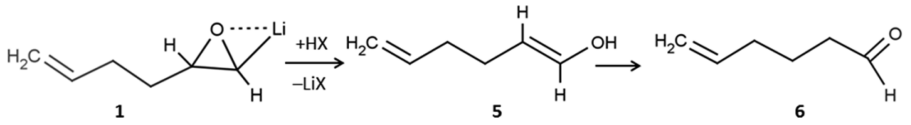

deviations. The full tables are provided in the Supporting Information. As noted above, the dimer exists in two diastereomeric forms, and each has two isomers. The free energies of activation $\Delta G^{\ddagger}$ and the reaction free energies $\Delta_r G°$ for the monomer and the four tetrasolvated dimeric species reacting with ethylene are summarized in Table 9.

The $\Delta G^{\ddagger}$ values in Table 9 show that the free energy of activation for the monomer and the dimers are relatively insensitive to the aggregation state. Comparisons of these $\Delta G^{\ddagger}$ values of the tetrasolvated dimers in Table 9 to the activation barriers for the *disolvated* dimers (i.e., one THF per Li; see Supporting Information, Table S6C) show that the barriers are also insensitive to solvation state. The dimer activation barriers in THF solution are comparable to those for the dimers in nonpolar medium (Table 7).

DISCUSSION

Our results indicate that the cyclopropanation reaction of methoxymethyllithium with ethylene proceeds exclusively by the carbolithiation pathway. Both MP2//DFT and CCSD-(T)//DFT predict higher reaction barriers for this reaction than that for the ethylene oxide monomer (compare Tables 1 and 2), which reacts exclusively by the concerted methylene transfer mechanism. THF solvation appears to have only a weak effect on the $\Delta G^{\ddagger}$ for both reagents in the monomeric form.

The intramolecular carbenoid reaction of **1** (Scheme 3, Figure 2) proceeds by the carbolithiation and methylene transfer pathways. However, the reaction barriers in the former pathway are less than half of the latter. It was found that other competing noncarbenoid reaction pathways are also possible, but these have reaction barriers that are of the same magnitude or even higher than the methylene transfer pathway.

Hodgson et al. report that in their room-temperature synthesis starting from **1**, the alcohol **4** was formed in 47% yield, and that "the volatile 5-hexenal was also observed" (yield unspecified).[19] The most plausible pathway from **1** to the aldehyde is the conversion of the unreacted lithiooxirane to the vinyl alcohol **5** during final workup and then, by keto−enol tautomerism, to the aldehyde **6**, as shown in Scheme 5. In the absence of a double bond in the vicinity, epoxyalkanes are known to give the corresponding aldehyde *exclusively* when treated with lithium 2,2,6,6-tetramethylpiperidide.[45] The formation of **6** from **5** is thermodynamically favorable, as indicated by the $\Delta_r G°$ calculated using M06-2X/6-31+G(d) of −13.8 kcal/mol.

There are at least two reactions competing with the formation of **4**. One is C_2 to C_1 hydrogen transfer in **1** leading to 5-hexene-2-one. The M06-2X/6-31+G(d) free energy barrier for this is 21.4 kcal/mol compared to 21.3 kcal/mol for the concerted methylene transfer reaction. The second is the rearrangement of **1** (breaking of the C_2−O bond) to yield the lithiated precursor of **5**, for which M06-2X/6-31+G(d) predicts a free energy barrier of 24.2 kcal/mol. Hodgson et al. report that the yield of **4** increases when temperature is lowered (62% at 0 °C in hexane),[19] which could be attributed to the competing reactions with higher barriers becoming exponentially less favorable (Arrhenius law) as temperature is lowered. It is highly likely that, because of the method of their preparation, the lithium atoms in the reagents may remain coordinated to THF ligands even in nonpolar solvents. However, as the results presented here show, THF coordination has only a weak effect on the reaction barriers.

As the foregoing discussion would suggest, reactions of lithiated epoxides are known to yield products other than those due to cyclopropanation, such as unsaturated alcohols, aldehydes, and ketones, often in appreciable yields.[3−5,46,47] A detailed investigation of these "noncarbenoid" reactions of oxiranes is being reported in a forthcoming paper from two authors of our group.[48]

It is instructive to compare the carbenoid reactions of lithiated oxiranes to those of haloalkyllithiums. Both intramolecular[49] and intermolecular[24,26] reactions of haloalkyllithium carbenoids with alkene double bonds have been studied computationally. In the case of the intramolecular cyclization reaction of a bromoalkyllithium carbenoid, Ke et al.[49] report that the methylene transfer pathway has free energy barriers of 7.5 to 10.0 kcal/mol, depending on the reactant complex and product, at the B3LYP/6-311(d,p) level of theory. The free energy barriers on the carbolithiation pathways for the same cases range from 15.4 to 22.9 kcal/mol. In these cases, the Lewis base assistance provided by the coordination of an O atom (part of a siloxy group present in the molecue) to the Li was cited as one of the key factors that helped lower the reaction barrier for the methylene transfer case.[49] However, in the present case of the intramolecular reaction of lithiated 1,2-epoxy-5-hexene, the carbolithiation pathway is favored over the methylene transfer pathway. As Figure 2 shows, the Lewis base

dx.doi.org/10.1021/jo301550y | J. Org. Chem. 2012, 77, 8605−8614

assistance from the O atom is present in both pathways, and the O−Li distances are actually greater in **TS 2** (Figure 2d) than **TS 1** (Figure 2b). Turning to the intermolecular reactions, methoxymethyllithium appears to react exclusively by the carbolithiation pathway with ethylene while oxiranyllithium exclusively follows the methylene transfer pathway. Comparing Figures 1 and 3, the degree of Lewis base assistance from the O−Li proximity appears to be comparable in both cases. Also, the natural charges from NPA analysis do not immediately suggest an explanation for why one pathway is preferred over the other in these cases. We conclude that the factors determining the energetics of organolithium carbenoid reactions remain to be fully understood.

In the intermolecular case, the relative stability of various aggregates has to be taken into consideration before a fair comparison can be made between the two types of carbenoids. In nonpolar media, oxiranyllithium exists as tetramers or higher aggregates while in THF solution, the preferred state appears to be the tetrasolvated dimer. This is qualitatively very similar to the case of haloalkyllithiums,[24] which also exist as tetrameric or higher aggregates in nonpolar solvents and as tetrasolvated dimers in THF solution. It is appropriate to compare the thermodynamics of oxiranyllithium cyclopropanation to those of the carbenoid species $LiCH_2OH$, which has been studied by Ke et al. using B3LYP/6-311G(d,p) method in the gas phase.[26] The *gas-phase* methylene transfer $\Delta G^{\ddagger}$ for cyclopropanation of ethylene using $LiCH_2OH$ monomer, dimer, and tetramer are 19.0, 18.9, and 19.9 kcal/mol, respectively,[26] compared to the B3LYP/6-31+G(d) nonpolar condensed-phase values from the present work, 18.3, 17.3 (*RS* dimer 2), and 13.3 (*RRSS*) kcal/mol, respectively (Supporting Information, Tables S5A and S5B). Applying standard state corrections, these yield *gas-phase* $\Delta G^{\ddagger}$ values of 20.2, 19.2, and 15.2 kcal/mol.

The dependence of the free energy barrier in the methylene transfer pathway to cyclopropanation in oxiranyllithium reported here follows the same pattern previously observed in the case of fluoro- and bromomethyllithiums.[24] For bromomethyllithium, the $\Delta G^{\ddagger}$ values for methylene insertion into the alkene double bond are 11.6, 10.5, and 8.3 kcal/mol, respectively, for the monomer, dimer, and tetramer, at the MP2//B3LYP level of treatment with the 6-31+G(d) basis set. The analogous activation barriers for oxiranyllithium are 19.3, 16.5, and 13.1 kcal/mol, respectively (see Supporting Information for MP2//B3LYP numbers). In each case, we have reported the lowest barrier for each aggregate in nonpolar solvent medium. In contrast to the case of halomethyllithiums, however, we have been unable to find evidence of a carbometalation pathway for oxiranyllithium.

SUMMARY AND CONCLUSION

This paper presents the first computational studies of the carbenoid cyclopropanation reactions of methoxymethyllithium and intramolecular and intermolecular carbenoid reactions of lithiated oxiranes. Computations suggest that methoxymethyllithium reacts with ethylene exclusively by a stepwise carbolithiation mechanism. The intramolecular reaction of lithiated 1,2-epoxy-5-hexene was found to proceed by both the carbolithiation and the methylene transfer pathways, but the former is expected to dominate at room and low temperatures because the free energy of activation is less than half that of the latter pathway. Other noncarbenoid pathways are also available in this case, leading to other products, and the free energies of activation for those are comparable to that of the methylene transfer pathway and higher than the carbolithiation pathway. The intermolecular cyclopropanation reactions of oxiranyllithium with ethylene, in contrast, appear to proceed exclusively by a concerted methylene transfer mechanism. Searches for carbometalation transition states in this case yielded structures that involve *intramolecular* hydrogen transfer within the oxirane reagent, with the alkene acting as a mere spectator. Thus the three cases studied represent the full spectrum of carbenoid cyclopropanation reaction mechanisms, exclusively carbolithiation to exclusively methylene transfer.

The activation free energy barriers for the methylene transfer reaction of lithioethylene oxide are comparable to those for lithiated methanol $LiCH_2OH$[26] and higher than those for fluoro- and bromomethyllithiums.[24,26] Dependence of the free energy of activation on the aggregation state of oxiranyllithium carbenoids is similar to those of bromomethyllithium carbenoids in that the barriers show downward trends as the aggregation size increases. However, compared to bromomethyllithium carbenoids, the barriers are uniformly higher for oxiranyllithium carbenoids for a given aggregate size, suggesting that halomethyllithium carbenoids are likely to be more efficient for cyclopropanation reactions under very mild conditions. In the case of both oxiranyllithiums and halomethyllithiums, nonpolar solvents are more favorable than polar solvents such as THF for the formation of higher aggregates which react with lower reaction barriers.

This work also accounted for the products observed and the temperature dependence of their distribution reported by Hodgson et al.[19] in the case of 1,2-epoxy-5-hexene as the result of competition between the carbenoids cyclopropanation reactions and noncarbenoid rearrangement reactions. Such noncarbenoid reactions which lead to allyl and vinyl alcohols, aldehydes, and ketones appear to be quite common among epoxides, as exemplified by the synthetic routes explored by Crandall and Chang.[3] A detailed computational study of such reactions will be described in a forthcoming report.[48]

ASSOCIATED CONTENT

Supporting Information

The complete data for Tables 2−5 and 7−9. The IRCs for the two carbenoid pathways in Figure 2. Converged M06-2X/6-31+G(d) structures of all molecules studied. This material is available free of charge via the Internet at http://pubs.acs.org.

AUTHOR INFORMATION

Corresponding Author

*E-mail: ramu@latech.edu.

Present Address

[§]Department of Chemistry, Kyung Hee University, 1 Seochun-Dong, Giheung-Gu, Yongin-Si, Gyeonggi-Do, 446−701, Korea.

Notes

The authors declare no competing financial interest.

ACKNOWLEDGMENTS

Support by the National Science Foundation through CHE-0643629, CHE-1049622, OISE-0744375, and EPS-1003897 is acknowledged. This work utilized the resources of the National Energy Research Center (NERSC), which is supported by the Office of Science of the Department of Energy under Contract No. DE-AC02-05CH11231. Grants of computer time from the Louisiana Optical Network Initiative (LONI) are gratefully acknowledged.

REFERENCES

(1) Satoh, T. *Chem. Rev.* **1996**, *96*, 3303.
(2) Capriati, V.; Florio, S.; Luisi, R.; Russo, V.; Salomone, A. *Tetrahedron Lett.* **2000**, *41*, 8835.
(3) Crandall, J. K.; Chang, L. H. *J. Org. Chem.* **1967**, *32*, 435.
(4) Crandall, J. K.; Chang, L. H. *J. Org. Chem.* **1967**, *32*, 532.
(5) Crandall, J. K.; Lin, L. H. C. *J. Am. Chem. Soc.* **1967**, *89*, 4527.
(6) Crandall, J. K.; Lin, L. H. C. *J. Am. Chem. Soc.* **1967**, *89*, 4526.
(7) Crandall, J. K.; Lin, L. H. C. *J. Org. Chem.* **1968**, *33*, 2375.
(8) Abbotto, A.; Capriati, V.; Degennaro, L.; Florio, S.; Luisi, R.; Pierrot, M.; Salomone, A. *J. Org. Chem.* **2001**, *66*, 3049.
(9) Concellón, J. M.; Bernad, P. L.; del Solar, V.; Suárez, J. R.; García-Granda, S.; Díaz, M. R. *J. Org. Chem.* **2006**, *71*, 6420.
(10) Nagaki, A.; Takizawa, E.; Yoshida, J. I. *J. Am. Chem. Soc.* **2009**, *131*, 1654.
(11) Morgan, K. M.; Gronert, S. *J. Org. Chem.* **2000**, *65*, 1461.
(12) Morgan, K. M.; O'Connor, M. J.; Humphrey, J. L.; Buschman, K. E. *J. Org. Chem.* **2001**, *66*, 1600.
(13) Hodgson, D. M.; Maxwell, C. R.; Wisedale, R.; Matthews, I. R.; Carpenter, K. J.; Dickenson, A. H.; Wonnacott, S. *J. Chemical. Soc., Perkin Trans. 1* **2001**, 3150.
(14) Hodgson, D. M.; Lee, G. P.; Marriott, R. E.; Thompson, A. J.; Wisedale, R.; Witherington, J. *J. Chemical. Soc., Perkin Trans. 1* **1998**, 2151.
(15) Gallagher, D. J.; Wu, S.; Nikolic, N. A.; Beak, P. *J. Org. Chem.* **1995**, *60*, 8148.
(16) Hodgson, D. M.; Lee, G. P. *Chem. Commun.* **1996**, 1015.
(17) Agami, C.; Dechoux, L.; Doris, E.; Mioskowski, C. *Tetrahedron Lett.* **1997**, *38*, 4071.
(18) Dechoux, L.; Agami, C.; Doris, E.; Mioskowski, C. *Eur. J. Org. Chem.* **2001**, 4107.
(19) Hodgson, D. M.; Chung, Y. K.; Paris, J. M. *J. Am. Chem. Soc.* **2004**, *126*, 8664.
(20) Xie, X.; Yue, G.; Tang, S.; Huo, X.; Liang, Q.; She, X.; Pan, X. *Org. Lett.* **2005**, *7*, 4057.
(21) Hodgson, D. M.; Ying, K. C.; Nuzzo, I.; Freixas, G.; Kulikiewicz, K. K.; Cleator, E.; Paris, J. M. *J. Am. Chem. Soc.* **2007**, *129*, 4456.
(22) Hodgson, D. M.; Salik, S.; Fox, D. J. *J. Org. Chem.* **2010**, *75*, 2157.
(23) Ramachandran, B. R.; Pratt, L. M. In *Practical Aspects of Computational Chemistry II*; Leszczynski, J., Shukla, M. K., Eds.; Springer: Dordrecht, 2012; p 471.
(24) Pratt, L. M.; Trần, P. T. T.; Nguyễn, N. V.; Ramachandran, B. *Bull. Chem. Soc. Jpn.* **2009**, *82*, 1107.
(25) Ramachandran, B.; Kharidehal, P.; Pratt, L. M.; Voit, S.; Okeke, F. N.; Ewan, M. *J. Phys. Chem. A* **2010**, *114*, 8423.
(26) Ke, Z.; Zhao, C.; Phillips, D. L. *J. Org. Chem.* **2007**, *72*, 848.
(27) Simmons, H. E.; Smith, R. D. *J. Am. Chem. Soc.* **1958**, *80*, 5323.
(28) Simmons, H. E.; Smith, R. D. *J. Am. Chem. Soc.* **1959**, *81*, 4256.
(29) Hoberg, H. *Justus Liebigs Ann. Chem.* **1962**, *656*, 1.
(30) Burger, U.; Huisgen, R. *Tetrahedron Lett.* **1970**, *11*, 3049.
(31) Stiasny, H. C.; Hoffmann, R. W. *Chem.—Eur. J.* **1995**, *1*, 619.
(32) Nakamura, M.; Hirai, A.; Nakamura, E. *J. Am. Chem. Soc.* **2003**, *125*, 2341.
(33) Frisch, M. J. T. G. W.; Schlegel, H. B.; Scuseria, G. E.; Robb, M. A.; Cheeseman, J. R.; Scalmani, G.; Barone, V.; Mennucci, B.; Petersson, G. A.; Nakatsuji, H.; Caricato, M.; Li, X.; Hratchian, H. P.; Izmaylov, A. F.; Bloino, J.; Zheng, G.; Sonnenberg, J. L.; Hada, M.; Ehara, M.; Toyota, K.; Fukuda, R.; Hasegawa, J.; Ishida, M.; Nakajima, T.; Honda, Y.; Kitao, O.; Nakai, H.; Vreven, T.; Montgomery, J. A., Jr.; Peralta, J. E.; Ogliaro, F.; Bearpark, M.; Heyd, J. J.; Brothers, E.; Kudin, K. N.; Staroverov, V. N.; Kobayashi, R.; Normand, J.; Raghavachari, K.; Rendell, A.; Burant, J. C.; Iyengar, S. S.; Tomasi, J.; Cossi, M.; Rega, N.; Millam, N. J.; Klene, M.; Knox, J. E.; Cross, J. B.; Bakken, V.; Adamo, C.; Jaramillo, J.; Gomperts, R.; Stratmann, R. E.; Yazyev, O.; Austin, A. J.; Cammi, R.; Pomelli, C.; Ochterski, J. W.; Martin, R. L.; Morokuma, K.; Zakrzewski, V. G.; Voth, G. A.; Salvador, P.; Dannenberg, J. J.; Dapprich, S.; Daniels, A. D.; Farkas, Ö.; Foresman, J. B.; Ortiz, J. V.; Cioslowski, J.; Fox, D. J. *Gaussian 09*, Rev. A.1. ed.; Gaussian Inc., Wallingford, CT, 2009.
(34) Pratt, L. M.; Ramachandran, B. *J. Org. Chem.* **2005**, *70*, 7238.
(35) Becke, A. D. *J. Chem. Phys.* **1993**, *98*, 1372.
(36) Lee, C.; Yang, W.; Parr, R. G. *Phys. Rev. B* **1988**, *37*, 785.
(37) Stephens, P. J.; Devlin, F. J.; Chabalowski, C. F.; Frisch, M. J. *J. Phys. Chem.* **1994**, *98*, 11623.
(38) Perdew, J. P.; Burke, K.; Ernzerhof, M. *Phys. Rev. Lett.* **1996**, *77*, 3865.
(39) Perdew, J. P.; Ernzerhof, M.; Burke, K. *J. Chem. Phys.* **1996**, *105*, 9982.
(40) Zhao, Y.; Truhlar, D. G. *Theor. Chem. Acc.* **2008**, *120*, 215.
(41) Gonzalez, C.; Bernhard Schlegel, H. *J. Chem. Phys.* **1989**, *90*, 2154.
(42) Gonzalez, C.; Schlegel, H. B. *J. Phys. Chem.* **1990**, *94*, 5523.
(43) Reed, A. E.; Weinstock, R. B.; Weinhold, F. *J. Chem. Phys.* **1985**, *83*, 735.
(44) Weinhold, F.; Carpenter, J. E. In *The Structure of Small Molecules and Ions*; Naaman, R., Vager, Z., Eds.; Plenum: New York, 1988, p 227.
(45) Yanagisawa, A.; Yasue, K.; Yamamoto, H. *J. Chem. Soc., Chem. Commun.* **1994**, 2103.
(46) Hodgson, D. M.; Fleming, M. J.; Stanway, S. J. *J. Am. Chem. Soc.* **2004**, *126*, 12250.
(47) Hodgson, D. M.; Humphreys, P. G.; Hughes, S. P. *Pure Appl. Chem.* **2007**, *79*, 269.
(48) Ramachandran, B. R.; Pratt, L. M. Manuscript in preparation..
(49) Ke, Z.; Zhou, Y.; Gao, H.; Zhao, C.; Phillips, D. L. *Chem.—Eur. J.* **2007**, *13*, 6724.